

Lifetime measurements in Tl III and the determination of the ground-state dipole polarizabilities for Au I–Bi V

M. Henderson, L. J. Curtis, R. Matulioniene, D. G. Ellis, and C. E. Theodosiou

Department of Physics and Astronomy, University of Toledo, Toledo, Ohio 43606

(Received 1 April 1997)

Measurements are reported for the lifetimes of the $6p\ ^2P_{1/2,3/2}$, $6d\ ^2D_{3/2,5/2}$, $7s\ ^2S_{1/2}$, $7p\ ^2P_{1/2,3/2}$, $7d\ ^2D_{5/2}$, and $5f\ ^2F_{5/2,7/2}$ levels in Tl III, made using beam-foil excitation. Theoretical calculations are also presented to elucidate conditions of configuration interaction exhibited by the measurements. In addition, values for the measured $6p$ lifetimes in the Au sequence are combined with theoretical calculations of resonance transitions to higher levels to specify the ground-state dipole polarizabilities for Au I, Hg II, Tl III, Pb IV, and Bi V. [S1050-2947(97)10609-6]

PACS number(s): 32.70.Cs

I. INTRODUCTION

The Au isoelectronic sequence is the heaviest member of the group IB coinage-metal-like homologs Cu, Ag, and Au, which have $(n-1)d^{10}ns\ ^2S_{1/2}$ ground states. Although these systems have a relatively simple electronic structure, they possess interesting subtleties. In all three sequences, the p and f series are affected by a strong configuration interaction (CI) with the d^9sp configuration [1–3]. In the Au sequence this mixing of the $5d^{10}np\ ^2P$ and $5d^{10}nf\ ^2F$ levels with the $5d^96s6p\ ^{2,4}PDF$ manifold opens additional decay channels to the metastable $5d^96s^2\ ^2D$ levels. The $5d^{10}6s-5d^{10}np$ transitions are (for $n>6$) subject to cancellation effects that are nearly complete for some cases. The $5d^{10}6s-5d^96s6p$ transitions provide an additional resonance excitation process that is not present in alkali-metal-like sequences, which contributes significantly to the ground state dipole polarizability α_d of the ion.

Lifetime measurements already exist for a variety of levels in Au I [4,5], Hg II [6–8], Pb IV [9,10], and Bi V [11], but only the lifetimes of the $6p$ and $5f$ levels have been reported until now for Tl III [12–15]. Theoretical calculations [16–18] have been made for a few selected transition probabilities in this sequence, but none have included the important $5d^96s^2$ or $5d^96s6p$ levels. The lifetimes of levels in the Tl III ion are interesting for a number of reasons. Tl has been observed in Hubble Space Telescope spectra of peculiar stars [19–21] that require oscillator strength data for their interpretation. Semiempirical studies [22] indicate that Tl III is the case where cancellation effects in the $6s-np$ oscillator strengths are the most severe, introducing large uncertainties in their theoretical specification. Through a theoretical accounting of these cancellations and other contributions to the ground state oscillator strengths, it is possible [23,24] to specify α_d from measurements of the $5d^{10}6p$ lifetimes. Naturally occurring Tl has two stable isotopes, ^{205}Tl (70.5%) and ^{203}Tl (29.5%), which both have nuclear spin $I=\frac{1}{2}$, and have been the object of studies of hyperfine structure [25] and of electroweak parity nonconserving optical rotation [26,27]. Comprehensive lifetime studies for these ions can also provide tests of theoretical methods that permit their extension to higher members of the Au sequence, which (except for

Th XII and U XIV) are radioactively unstable. The spectroscopic inaccessibility of these unstable ions does not lessen the importance of their atomic properties in practical applications. For example, the atomic rate constants can enter the dynamical modeling of a fusion plasma on a time scale that is much shorter than either the atomic mean life or the nuclear disintegration time.

The accurate determination of ground-state polarizabilities for ions in the Au sequence is valuable since it provides a means for predicting and identifying transitions among high Rydberg states in the Hg sequence. The energy levels [28] and transition probabilities [29] of these nonpenetrating states can be described accurately by the core polarization model, which treats the system as a single outer electron in the presence of the polarized core of the next stage of ionization. Such states are often very strongly populated in low density light sources in which they are not Stark quenched by interionic fields.

We report here lifetime measurements for the $5d^{10}6p$, $6d$, $7s$, $7p$, $7d$, and $5f$ levels in Tl III, together with theoretical calculations for the transition probabilities of these and the $5d^96s6p$ levels in this ion. We also report a determination of the ground-state dipole polarizabilities for the ions Au I–Bi V, obtained by combining available lifetime measurements for the $5d^{10}6p$ levels with theoretical estimates of other oscillator strengths that contribute to this quantity. These studies provide both quantitative specification and qualitative insights into the subtleties that characterize the coinage-metallike sequences and contrast them with the alkali-metal-like sequences.

II. CALCULATIONAL FORMULATION

A. Theoretical calculations

In order to interpret our lifetime measurements, help assess any potential problems with blends and cascades, and relate our results to oscillator strengths and polarizabilities, we have carried out calculations for the sequence of spectra Au I–Bi V using the set of programs RCN-RCG-RCE by Cowan [30]. Although not necessarily the method for computing the best possible *ab initio* value for a given transition probability, the Cowan program suite offers a combination of fea-

tures that makes it a powerful tool in connection with laboratory work in atomic spectroscopy. Our calculations were done in intermediate coupling, using the HFR (Hartree-Fock with relativistic corrections) mode; the most important configuration interactions were included explicitly, and the default scaling of Slater integrals was used to give a rough indication of the remaining CI effects. In addition we made a limited number of empirical adjustments to improve the agreement between computed and observed energy levels.

For the case of Tl III, we used 8 even-parity ($6s, 7s, 8s, 6s^2, 6d, 7d, 6p^2, 5g$) and 4 odd-parity ($6p, 7p, 6s6p, 5f$) configurations. For the even configurations we made empirical adjustments of the configuration-average energies ($\leq 5\%$), and of the three nd spin-orbit integrals ($\leq 2 \text{ cm}^{-1}$). For the odd configurations we did a complete least-squares fit, varying 22 parameters (4 average energies, 5 Slater integrals, 8 CI integrals, and 5 spin-orbit integrals) to fit the 23 observed energy levels. The rms disagreement between calculated and observed energies decreased from about 3% to less than 0.2% as a result of the fit. For Pb IV and Bi V we used exactly the same procedure, obtaining similar results.

For Au I and Hg II, the number of configurations that must be included is greater, and conditions are not as favorable for a least-squares fit, which requires a small number of configurations, relatively isolated from others, with completely known energy levels. In these two cases we used 9 even configurations (those listed above plus $6s7s$), and 10 odd configurations (the above plus $8p, 9p, 10p, 6s7p, 6s5f, 6s^26p$). Empirical adjustments were made only for the configuration-average energies and for the $5d$ and $6p$ spin-orbit integrals.

B. Cancellation effects

Systematic cancellation effects are well known to occur in intershell transitions in alkali-metallike and coinage-metallike isoelectronic sequences [31]. For $ns-n'p$ ($n' > n$) transitions, cancellations of this type occur for Mg II [23,32] in the Na sequence; Ca II [23] in the K sequence; Zn II [24], Ga III in the Cu sequence; Cd II, In III, Sn IV in the Ag sequence; and Hg II, Tl III, Pb IV in the Au sequence [22]. These effects can be traced using a quantum defect formalism [31] in which regions outside the core are characterized by a hydrogenlike wave function of shifted phase. The phase shifts associated with penetration and with polarization differ in their dependences on the core charge, and differential shifts between the upper and lower state wave functions cause the dipole transition integral to undergo systematic sign changes at particular values of the effective quantum numbers.

This type of cancellation is illustrated in Fig. 1, which plots the effective quantum numbers obtained from measured spectroscopic data for the Au sequence together with the theoretically predicted nodal lines of cancellation. Experimental studies have shown that lifetime and relative intensity anomalies exist for the $7p \ ^2P_{1/2}$ and $\ ^2P_{3/2}$ levels in Hg II [7] and Pb IV [10], consistent with the proximity of the $6s-7p$ transitions (particularly for the $\ ^2S_{1/2}-\ ^2P_{1/2}$ case) to the line of cancellation nodes in Fig. 1. Because of these cancellations, the major channels for resonance absorption of radiation are

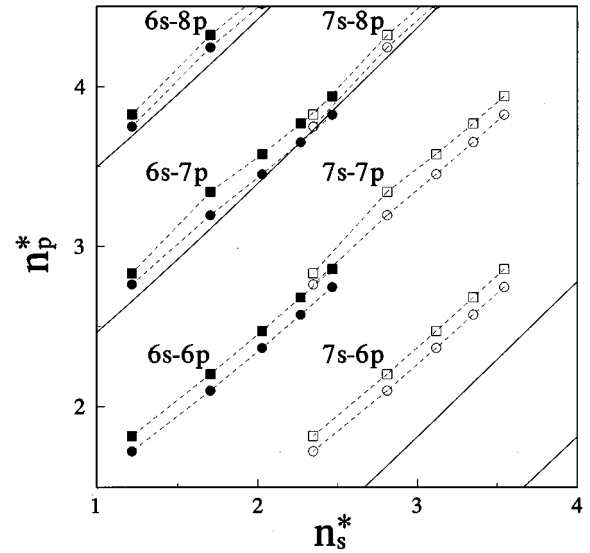


FIG. 1. Cancellation plot of the Au sequence. Solid lines indicate theoretically predicted nodes in the transition integral. Symbols denote experimental effective quantum numbers for the $6s \ ^2S_{1/2}-np \ ^2P_{1/2}$ (filled circles), $6s \ ^2S_{1/2}-np \ ^2P_{3/2}$ (filled squares), $7s \ ^2S_{1/2}-np \ ^2P_{1/2}$ (open circles), $7s \ ^2S_{1/2}-np \ ^2P_{3/2}$ (open squares).

expected to be via the $5d^{10}6s-5d^{10}6p$ and $5d^{10}6s-5d^96s6p$ transitions.

C. Dipole polarizabilities

Precision lifetime measurements for the $5d^{10}6p$ levels in these ions can be combined with calculations of the oscillator strengths of both of the $5d^{10}6s-5d^{10}np$ ($n > 6$) and $5d^{10}6s-5d^96s6p$ transitions and used to specify α_d , using the expression

$$\alpha_d = \sum_{J=\frac{1}{2}, \frac{3}{2}} [\alpha_{d0} + \Delta\alpha_{db} + \Delta\alpha_{db'} + \Delta\alpha_{dc}], \quad (1)$$

where α_{d0} involves the intrashell $6s-6p$ resonance transitions

$$\alpha_{d0} = (2\mathcal{R}\lambda_{6s,6p})^2 f_{6s,6p}, \quad (2)$$

$\Delta\alpha_{db}$ involves the intershell bound-bound resonance transitions to singly excited levels

$$\Delta\alpha_{db} = \sum_{n>6} (2\mathcal{R}\lambda_{6s,np})^2 f_{6s,np}, \quad (3)$$

$\Delta\alpha_{db'}$ involves the bound-bound resonance transition channels to doubly excited levels

$$\Delta\alpha_{db'} = \sum_{6s6p} (2\mathcal{R}\lambda_{6s,6s6p})^2 f_{6s,6s6p}, \quad (4)$$

and $\Delta\alpha_{dc}$ involves the bound-free continuum transitions

$$\Delta\alpha_{dc} = (2\mathcal{R})^2 \int_0^\infty dE \frac{df/dE}{(E+I_0)^2}. \quad (5)$$

Here $f_{6s,np}$ and $f_{6s,6s6p}$ are the absorption oscillator strengths for the $5d^{10}6s^2S_{1/2}-5d^{10}np^2P_J$ and $5d^{10}6s^2S_{1/2}-5d^96s6p^{2,2,4}PDF_J$ transitions with the corresponding wavelengths $\lambda_{6s,np}$ and $\lambda_{6s,6s6p}$ (with J implicit in the notation). I_0 is the ionization potential of the ground state, and \mathcal{R} is the Rydberg constant.

If Eq. (1) is dominated by the α_{d0} term, α_d can be deduced from the wavelength and oscillator strength data for the intrashell $6s-6p$ transitions alone. If those transitions are unbranched or have accurately known branching fractions $B_{6s,6p}$, the oscillator strengths can be obtained from the measured lifetimes τ_{6p} of the $5d^{10}6p^2P_J$ levels using

$$f_{6s,6p} = \left[\frac{\lambda_{6s,6p}(\text{\AA})}{2582.7} \right]^2 \frac{(J + \frac{1}{2})B_{6s,6p}}{\tau_{6p}(ns)}. \quad (6)$$

In this case the uncertainties in the determination can be estimated by propagating the quoted uncertainties in the lifetime measurements and branching fraction determinations to obtain the uncertainty $\delta\alpha_{d0}$ in α_{d0} , and combining this with estimates of the magnitudes and tolerances in the theoretical specification of the $n > 6$ and $6s6p$ transitions. Assuming that the uncertainties in the contributions from the higher singly excited bound states and the continuum are uncorrelated and not larger than the contributions themselves, and that the calculations for the doubly excited states are accurate to at least 50%, the uncertainty $\Delta\alpha_d$ in the determination of α_d is given by

$$\Delta\alpha_d^2 = \sum_{J=\frac{1}{2}, \frac{3}{2}} [\delta\alpha_{d0}^2 + \Delta\alpha_{db}^2 + \frac{1}{4}\Delta\alpha_{db'}^2 + \Delta\alpha_{dc}^2]. \quad (7)$$

Uncertainty limits on the contributions due to higher terms could also be estimated by combining the deficiency from the f -sum rule, the energy of the highest level included in sum, and the fact that all oscillator strengths from the ground state are positive. However, in the present case, departures from the single active electron sum rule are expected to arise due to the existence of open subshells and core polarization effects.

Theoretical estimates of the contributions of higher n transitions were made using extrapolated energy level data and two implementations of the semiempirical Coulomb approximation. One method [33] uses a small r cutoff, whereas the other [23] uses the Coulomb approximation with a central potential (CACP) to represent the core. The available measured spectroscopic data for the $5d^{10}6s$ ionization potential and the $5d^{10}np$ excitation energies E_n for Au I [34,35], Hg II [36,37], Tl III [25,38], Pb IV [38], and Bi V [39] were reduced to effective quantum numbers n_p^* using

$$n_p^* \equiv \zeta \sqrt{\frac{\mathcal{R}}{I_0 - E_n}}, \quad (8)$$

where ζ denotes the isoelectronic charge state. These were parametrized by a Ritz quantum defect expansion

$$n - n_p^* = a + b/n_p^{*2} + c/n_p^{*4} + \dots, \quad (9)$$

which was least squares fitted and iterated to predict energy levels up to $n=50$. From these energies, values for $f_{6s,np}$ were explicitly calculated for $n \leq 50$. These results were extrapolated from $n=51$ to ∞ both through the use of a Padé approximation and by fitting the values of $f_{6s,np}\lambda_{6s,np}^2$ in the region $n=30-50$ to a low order polynomial in $1/n_p^{*3}$, which was summed to $n=\infty$ through the use of the Riemann zeta function [40]. The results obtained by the two implementations of the Coulomb approximations were essentially consistent, and the CACP results were selected for use in this application. The oscillator strengths for the $5d^{10}6s-5d^96s6p$ transitions were computed by use of the Cowan program [30]. Finally, the transitions to continuum states up to about 500 eV above threshold were calculated using the Hartree-Slater (HS) approach of Ref. [41], including relativistic and core polarization effects as in Ref. [23]. The values were combined using Eqs. (1) and (7) to obtain $\alpha_d \pm \Delta\alpha_d$.

III. EXPERIMENT

A. Measurements

The measurements utilized the 300-kV University of Toledo Heavy Ion Accelerator. Detailed descriptions of this facility can be found in reports of earlier studies (e.g., [42,43]) as well as in instrumentation reviews [44,45]. Ions of Tl^{2+} were produced in the ion source, accelerated through 20 kV, and magnetically analyzed. After momentum and mass-to-charge selection, the doubly charged ions were postaccelerated through an additional 220 kV to final energies of 480 keV. The ions then entered an electrostatic switchyard and were steered into the experimental station and collimated before passage through a thin ($2.1-2.5 \mu\text{g}/\text{cm}^2$) carbon foil. At beam energies of 480 keV, the observed spectroscopic excitations were primarily in Tl II, Tl III, and Tl IV [46].

The Tl III emission lines were analyzed with an Acton 1-m normal incidence vacuum ultraviolet monochromator, with three sets of concave gratings and detectors: a 2400-line/mm grating coupled with a channeltron detector below 1150 Å (for the $7p$ and $7d$ transitions); a 1200-line/mm grating coupled with a solar blind detector for 1150–1850 Å (for the $6p$, $6d$, and $7s$ transitions); and a 600-line/mm grating coupled with a bialkali detector for 2200–4500 Å (for the $5f$ transitions). The 1200-line/mm grating with the bialkali detector provides access to 1850–2200 Å, but none of these transitions occurs in that region. The post foil velocity was determined to within 2.5% by taking into account uncertainties in the energy calibration, the foil thickness [47], and possible beam divergence effects [48].

Using the Danfysik Model 911A ion source, ions were obtained from pure thallium metal. To minimize foil breakage, the current was limited to less than 200 nA (100-particle nA for Tl^{2+}). Currents of Tl^{2+} greater than 200 nA could be obtained with relative ease, and it was possible to achieve currents approaching 1 μA . The methods used to obtain doubly charged ions in the source are similar to those described earlier [42,43].

B. Data analysis

Due to the nonselective nature of beam-foil excitation, the level populations (and hence the decay curves) are affected

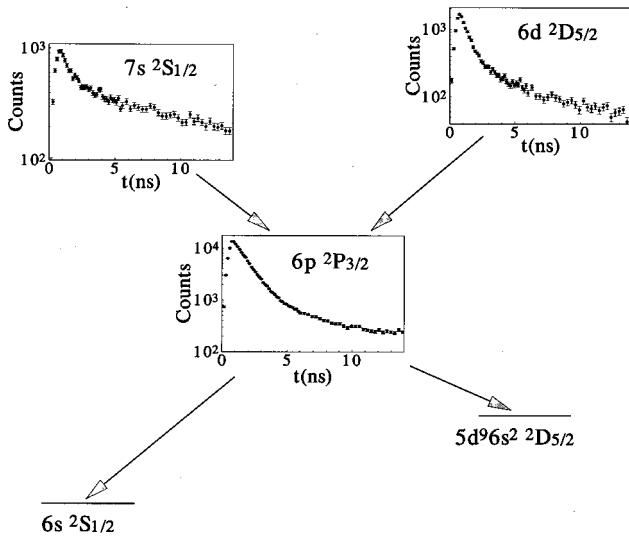


FIG. 2. Schematic representation of the ANDC method as applied to the decay curves of the $6p$ level and its cascades from $6d$ and $7s$. Using Eq. (10), each value of t_i provides a separate relationship by which the primary lifetime and the relative normalizations of the cascade decay can be determined.

by cascade repopulation. Thus, while they produce a negligible contribution in the case of long-lived decays, cascades can substantially distort the decay curves of shorter-lived levels. Situations in which cascading is dominated by a few strong decay channels are ideally suited to the arbitrarily normalized decay curve (ANDC) method [49,50]. This method performs a correlated analysis of the decay curves of the primary level and those of the levels that directly repopulate it, and yields both the primary lifetime and the intensity normalizations of the cascades relative to that of the primary.

A schematic representation of the ANDC method is shown in Fig. 2, indicating that the arbitrarily normalized decay curves $I_{nl}(t)$ of the $6p$ ${}^2P_{3/2}$ level and its cascades from the $6d$ ${}^2D_{5/2}$ and $7s$ ${}^2S_{1/2}$ are jointly analyzed using the population equation in the form

$$\tau_{6p} \frac{dI_{6p}}{dt}(t_i) = \xi_{6d} I_{6d}(t_i) + \xi_{7p} I_{7p}(t_i) - I_{6p}(t_i). \quad (10)$$

Here the lifetime τ_{6p} of the $6p$ level and the relative normalizations ξ_{nl} for the cascades and primary decay curves are determined by simultaneous solution of the large set of relationships provided by Eq. (10) evaluated at each of the common points t_i on the decay curves.

All decay curves were first analyzed by the multiexponential fitting program DISCRETE [51]. Next, ANDC analyses were attempted for the $6p$, $6d$, and $7s$ levels. Two ANDC codes were used: one employs numerical differentiation of the raw data; the other utilizes the program CANDY [52], which smooths the data through the application of a multiexponential filter. Uncertainties were computed by combining statistical uncertainties in the individual fits, scatter among the independent measurements, and estimates of possible errors introduced by cascade corrections.

IV. RESULTS

Our measured lifetime results are presented in Table I, together with comparisons to earlier measurements

[12,13,15], to our theoretical calculations made using the Cowan program [30], and to earlier calculations [16–18].

The lifetimes reported are all consistent with our curve fitted values, but in the cases of the two $6p$ and one of the $6d$ levels, the ANDC yielded improved accuracy and dynamical consistency among the various correlated decay curves, and were selected for presentation here. For the $6p$ ${}^2P_{3/2}$ level, the ANDC analysis (shown in Fig. 2) indicated significant repopulation from the $7s$ ${}^2S_{1/2}$, $6d$ ${}^2D_{5/2}$, and $7d$ ${}^2D_{5/2}$ levels. The other ANDC analyses indicated that the primary repopulation of the levels were as follows: for $6p$ ${}^2P_{1/2}$ by $7s$ ${}^2S_{1/2}$; for $6d$ ${}^2D_{3/2}$ by $7p$ ${}^2P_{1/2}$, and for $6d$ ${}^2D_{5/2}$ by $5f$ ${}^2F_{7/2}$. This difference in repopulation dynamics within the fine structure of the $6d$ levels occurs because of the J dependence of the CI-induced branching of the $7p$ and $5f$ levels to the $5d^9 6s^2$ levels. For this reason and because the ANDC procedure indicated large uncertainties for that case, we have adopted the curve fit value rather than the ANDC value for the $6d$ ${}^2D_{5/2}$ lifetime. For the $7s$ level, the np cascade transitions are all weak (since they are either intrashell or in nearly exact cancellation), hence the long tail exhibited in its decay curve in Fig. 2 must arise from CI-induced cascading from the $5d^9 6s 6p$ $J = \frac{1}{2}$ and $\frac{3}{2}$ levels that exist above it. Correspondingly, the ANDC analysis of $7s$ with $7p$ indicated no decay curve correlation.

The J dependences of the lifetime results for the $7p$ and $5f$ levels are particularly interesting. In the case of the $7p$ levels, very large J dependences (12:1 and 6:1) have been observed for the isoelectronic ions Hg II [7] and Pb IV [10], caused primarily by sensitivity to the conditions of nearly exact cancellation of the $6s$ - $7p$ transitions. Although similar cancellation effects occur for Tl III, here the measured $7p$ lifetimes are nearly equal. In contrast the $5f$ levels exhibit a 12:1 measured lifetime ratio. To investigate this we have carried out CI calculations using the Cowan code [30] for the transition probabilities of these levels, which are summarized in Table II.

The effects of CI on these systems are interesting to note. The $7p$ transitions to ground are (as shown in Fig. 1) severely affected by cancellation. While producing an anomalous lifetime ratio in Hg II and Pb IV, in Tl III this cancellation causes the transitions to ground to be weak in intensity, but their lifetimes seem to be primarily determined by strong CI-quenched decay channel to the metastable $5d^9 6s^2$ levels. Although a discrepancy still exists between the measured and theoretical values shown in Table I, the calculations presented in Table II indicate the importance of these CI channels, and underscore the need for their experimental determination.

As shown in Table II, the origin of the J dependence of the $5f$ lifetime lies in a similar CI mixing between the $5d^9 6s 6p$ and $5d^{10} 5f$ level. This shortens the lifetime of the ${}^2F_{5/2}$ by opening an additional decay channel to $5d^9 6s^2$, and lengthens the lifetime of the ${}^2F_{7/2}$ by diminishing the purity of its $5f$ content.

The results of our determination of the dipole polarizabilities are given in Table III. Experimental measurements for the $6p$ lifetimes and branching fractions are listed, together with our CACP calculations for the lifetimes and, where needed, our HFR calculations for the branching fractions. Our branching fraction calculations agree well with the mea-

TABLE I. Measured and computed lifetimes in Tl III.

Level	λ (Å)	τ (ns)						
		Measured		Theoretical				
		This work	Others	This work	Others			
				HFR	CACP			
$6p\ ^2P_{1/2}$	1558.63	1.95 ± 0.06^a	1.8 ± 0.2^b	1.05	1.69	$1.21,^c$	$1.86,^d$	2.02^e
$6p\ ^2P_{3/2}$	1266.24	1.06 ± 0.04^a	$0.9 \pm 0.2,^b$	0.57	0.89	$0.66,^c$	$0.96,^d$	1.02^e
$6d\ ^2D_{3/2}$	1231.48	0.54 ± 0.06^a	0.75 ± 0.08^f	0.33	0.52	$0.46,^c$	$0.36,^g$	0.31^h
$6d\ ^2D_{5/2}$	1477.06	0.71 ± 0.03		0.53	0.64	$0.57,^c$	$0.49,^g$	0.52^h
$7s\ ^2S_{1/2}$	1659.93	0.83 ± 0.09		0.57	0.77	$0.83,^c$	$1.2,^g$	0.91^h
$7p\ ^2P_{1/2}$	633.46	0.98 ± 0.12		1.60				6.26^c
$7p\ ^2P_{3/2}$	611.47	0.97 ± 0.06		0.21				1.82^c
$7d\ ^2D_{3/2}$	818.29			1.19				1.03^c
$7d\ ^2D_{5/2}$	926.06	3.02 ± 0.26		1.44				1.35^c
$5f\ ^2F_{5/2}$	3164.55	0.41 ± 0.10	1.0 ± 0.3^c	0.46				1.86^c
$5f\ ^2F_{7/2}$	3457.43	4.92 ± 0.50	$5.0 \pm 1.0,^c$	2.01				2.32^c
$6s6p\ ^2P_{1/2}$	572.85			0.16				
$6s6p\ ^2P_{3/2}$	640.88			0.21				
$6s6p\ ^2P_{1/2}$	662.28			0.22				
$6s6p\ ^2P_{3/2}$	668.48			0.39				

^aANDC measurement.^bPoulsen *et al.*, Ref. [12].^cLindgård *et al.*, Ref. [13].^dBrage *et al.*, Ref. [16].^eMigdalek and Baylis, RHF with core pol., Ref. [17].^fAndersen *et al.*, Ref. [14].^gMigdalek, Ref. [18], rel.^hMigdalek, Ref. [18], nonrel.ⁱShimon and Endevidi, Ref. [15].

sured values [5] for Au I, and it was assumed that our calculations are accurate to within their deficiency from unity in the other three cases where branching is possible. Since the $6p$ lifetimes for Au I appear to be significantly affected by CI, the CACP values were omitted from Table III for that case.

The various contributions to α_d are presented individually and summed in Table III. In all cases the dominant contribution to α_d comes from the $6s$ - $6p$ oscillator strengths. Because of the fortuitous conditions of cancellation, the contributions of the bound-bound and bound-continuum singly excited transitions are relatively minor, and the largest uncertainties arise from experimental determinations of the $6p$ lifetimes and the theoretical estimates of the oscillator

TABLE II. Theoretical transition probabilities in Tl III for $5d^{10}nl$ levels with significant decay channels to the $5d^96s^2$ metastable levels.

Transition	$J-J'$	λ (Å)	A_{ik} (ns^{-1})			$J-J'$	λ (Å)	A_{ik} (ns^{-1})		
			HFR ^a	Coul. ^b	CACP ^c			HFR ^a	Coul. ^b	CACP ^c
7p branching										
$6s\ ^2S_J - 7p\ ^2P_{J'}$	1/2-1/2	633.5	0.465	0.029	0.013	1/2-3/2	611.5	3.265	0.311	0.067
$7s\ ^2S_J -$	1/2-1/2	5363.2	0.097	0.106	0.101	1/2-3/2	4111.5	0.137	0.213	0.206
$6d\ ^2D_J -$	3/2-1/2	7999.1	0.030	0.034	0.036	3/2-3/2	5501.9	0.006	0.008	0.008
						5/2-3/2	5929.8	0.043	0.065	0.069
$6s^2\ ^2D_J -$	3/2-1/2	1364.9	0.033			3/2-3/2	1267.7	0.009		
						5/2-3/2	1030.9	1.346		
5f branching										
$6d\ ^2D_J - 5f\ ^2F_{J'}$	5/2-5/2	3301.8	0.013	0.033	0.030	5/2-7/2	3457.4	0.410	0.438	0.036
	3/2-5/2	3164.5	0.195	0.511	0.052					
$6s^2\ ^2D_J -$	5/2-5/2	905.6	0.086			5/2-7/2	916.9	0.087		
	3/2-5/2	1082.6	1.863							

^aCowan code calculation [30].^bCoulomb approximation with cutoff [33].^cCoulomb approximation with core potential [41].

TABLE III. Determination of dipole polarizabilities from the dominant contributions of the measured $6p$ lifetimes and theoretical estimates of the magnitude of other contributions.

Ion	Transition	τ_{6p} (ns)		$B_{6s,6p}$	α_{d0}	$\Delta\alpha_{db}$	$\Delta\alpha_{db'}$	$\Delta\alpha_{dc}$	$\alpha_d(a_0^3)$
		Expt.	CACP ^a						
Au I	1/2-1/2	6.2 ± 0.2 , ^d	6.0 ± 0.1 ^e	0.98 ± 0.01 ^e	6.18 ± 0.09	0.027	4.04	0.245	30 ± 4
	1/2-3/2	4.7 ± 0.2 , ^d	4.6 ± 0.2 ^e	0.911 ± 0.004 ^e	11.93 ± 0.36	0.031	7.72	0.233	
Hg II	1/2-1/2	2.91 ± 0.11 ^f	2.88	1.0000 ^b	3.53 ± 0.13	0.010	2.02	0.034	15 ± 2
	1/2-3/2	1.80 ± 0.08 ^f	1.73	0.9937 ^b	5.98 ± 0.27	0.008	3.41	0.034	
Tl III	1/2-1/2	1.95 ± 0.06 ^g	1.69	1	2.19 ± 0.07	0.024	0.97	0.017	8.1 ± 0.9
	1/2-3/2	1.06 ± 0.04 ^g	0.89	1.0000 ^b	3.50 ± 0.13	0.007	1.40	0.015	
Pb IV	1/2-1/2	1.11 ± 0.01 ^h	1.13	1	1.93 ± 0.17	0.014	0.60	0.005	6.6 ± 0.6
	1/2-3/2	0.52 ± 0.04 ^h	0.54	1	3.11 ± 0.24	0.004	0.92	0.005	
Bi V	1/2-1/2	0.88 ± 0.10 ⁱ	0.82	1	1.38 ± 0.16	0.009	0.45	0.002	5.3 ± 0.5
	1/2-3/2	0.301 ± 0.016 ⁱ	0.36	1	2.68 ± 0.14	0.003	0.81	0.002	

^aCoulomb approximation with core potential [23].

^bCowan code calculation [30].

^cHartree-Slater calculation [41].

^dGaarde *et al.*, Ref. [4].

^eHannaford *et al.*, Ref. [5].

^fPinnington *et al.*, Ref. [6].

^gThis work.

^hAnsbacher *et al.*, Ref. [9].

ⁱAnsbacher *et al.*, Ref. [11].

strengths for $5d^{10}6s-5d^96s6p$ transitions. If measurements for the $6p$ lifetimes of improved accuracy became available, they could be incorporated into these calculations to produce values for α_d of correspondingly improved accuracy.

ACKNOWLEDGMENTS

This work was supported by the U.S. Department of Energy, Fundamental Interactions Branch, Office of Basic Energy Sciences, Division of Chemical Sciences, under Grant No. DE-FG02-94ER14461.

- [1] H. Beutler, *Z. Phys.* **84**, 289 (1933); **86**, 710 (1933).
 [2] W. C. Martin and J. Sugar, *J. Opt. Soc. Am.* **59**, 1266 (1969).
 [3] J. Carlsson, *Phys. Rev. A* **38**, 1702 (1988).
 [4] M. B. Gaarde, R. Zerne, L. Caiyan, J. Zhankui, J. Larsson, and S. Svanberg, *Phys. Rev. A* **50**, 209 (1994).
 [5] P. Hannaford, P. L. Larkins, and R. M. Lowe, *J. Phys. B* **14**, 2321 (1981).
 [6] E. H. Pinnington, W. Ansbacher, J. A. Kernahan, T. Ahmad, and Z.-Q. Ge, *Can. J. Phys.* **66**, 960 (1988).
 [7] S. T. Maniak, L. J. Curtis, R. E. Irving, I. Martinson, and R. Hellborg, *Phys. Lett. A* **182**, 114 (1993).
 [8] K. Blagoev *et al.*, *Phys. Rev. A* **37**, 4679 (1988); *Phys. Lett.* **106A**, 249 (1984); **117**, 185 (1986).
 [9] W. Ansbacher, E. H. Pinnington, and J. A. Kernahan, *Can. J. Phys.* **66**, 402 (1988).
 [10] E. H. Pinnington, W. Ansbacher, A. Tauheed, and J. A. Kernahan, *Can. J. Phys.* **69**, 594 (1991).
 [11] W. Ansbacher, E. H. Pinnington, A. Tauheed, and J. A. Kernahan, *Phys. Scr.* **40**, 454 (1989).
 [12] O. Poulsen, T. Andersen, S. M. Bentzen, and I. Koleva, *Nucl. Instrum. Methods Phys. Res.* **202**, 139 (1982).
 [13] A. Lindgård, S. Mannervik, B. Jelenkovic, and E. Veje, *Nucl. Instrum. Methods Phys. Res.* **202**, 59 (1982); *Z. Phys. A* **301**, 1 (1981).
 [14] T. Andersen, A. Kirkegård Nielsen, and G. Sørensen, *Phys. Scr.* **6**, 122 (1972).
 [15] L. L. Shimon and N. M. Erdevdi, *Opt. Spectrosc.* **42**, 137 (1977).
 [16] T. Brage, D. S. Leckrone, and C. Froese Fischer, *Phys. Rev. A* **53**, 192 (1996).
 [17] J. Migdalek and W. E. Baylis, *J. Quant. Spectrosc. Radiat. Transf.* **22**, 113 (1979).
 [18] J. Migdalek, *Can. J. Phys.* **54**, 130 (1976).
 [19] D. S. Leckrone, S. G. Johansson, G. Kalus, G. M. Wahlgren, and T. Brage, *Astrophys. J.* **462**, 937 (1996).
 [20] S. G. Johansson, G. Kalus, T. Brage, D. S. Leckrone, and G. M. Wahlgren, *Astrophys. J.* **462**, 943 (1996).
 [21] D. S. Leckrone, S. Johansson, G. M. Wahlgren, C. R. Proffitt, and T. Brage, *Phys. Scr.* **T65**, 110 (1996).
 [22] L. J. Curtis, *Can. J. Phys.* **69**, 668 (1991).
 [23] C. E. Theodosiou, L. J. Curtis, and C. A. Nicolaidis, *Phys. Rev. A* **52**, 3677 (1995).
 [24] L. J. Curtis and C. E. Theodosiou, *J. Opt. Soc. Am. B* **12**, 175 (1995).
 [25] Y. N. Joshi and A. J. J. Raassen, *Can. J. Phys.* **68**, 195 (1990).
 [26] N. H. Edwards, S. J. Phipp, P. E. G. Baird, and S. Nakayama, *Phys. Rev. Lett.* **74**, 2654 (1995).
 [27] P. A. Vetter, D. M. Meekhof, P. K. Majumder, S. K. Lamoreaux, and E. N. Fortson, *Phys. Rev. Lett.* **74**, 2658 (1995).
 [28] B. Edlén, in *Spektroskopie I*, edited by S. Flügge, *Handbuch der Physik* Vol. 27 (Springer, Berlin, 1964), pp. 80–220.
 [29] L. J. Curtis, *J. Phys. B* **12**, L509 (1979).
 [30] R. D. Cowan, *The Theory of Atomic Structure and Spectra* (University of California Press, Berkeley, 1981).
 [31] L. J. Curtis and D. G. Ellis, *J. Phys. B* **11**, L543 (1978).

- [32] Professor Bengt Edlén recalled to L.J.C. that his first postdoctoral assignment in the laboratory of Friedrich Paschen in the 1930s was to ascertain whether the as yet unobserved lines from the $3s$ - $4p$ transitions in Mg^+ were rigorously absent. Through a very long exposure, he photographed the lines despite their strong cancellation effects.
- [33] C. E. Theodosiou, Coulomb Approximation Program CAMATREL (unpublished).
- [34] J. C. Ehrhard and S. P. Davis, *J. Opt. Soc. Am.* **61**, 1342 (1971).
- [35] C. M. Brown and M. L. Ginter, *J. Opt. Soc. Am.* **68**, 243 (1978).
- [36] C. E. Moore, *Atomic Energy Levels*, Natl. Bur. Stand. Ref. Data. Ser., Natl. Bur. Stand. (U.S.) Circ. No. 35 (U.S. GPO, Washington, D.C., 1958), Vol. III (reissued 1971).
- [37] J. Reader and C. J. Sansonetti, *Phys. Rev. A* **33**, 1440 (1986).
- [38] F. Gutmann and A. M. Crooker, *Can. J. Phys.* **51**, 1823 (1973).
- [39] A. J. J. Raassen, A. A. van der Valk, and Y. N. Joshi, *J. Phys. B* **22**, 13 (1989).
- [40] E. Jahnke and F. Emde, *Table of Functions with Formulae and Curves* (Dover, New York, 1945), pp. 269–274.
- [41] C. E. Theodosiou, *Phys. Rev. A* **37**, 1795 (1988).
- [42] M. Henderson and L. J. Curtis, *J. Phys. B* **29**, L629 (1996).
- [43] M. Henderson, P. Bengtsson, J. Corcoran, L. J. Curtis, R. E. Irving, and S. T. Maniak, *Phys. Scr.* **53**, 309 (1996).
- [44] R. R. Haar, D. J. Beideck, L. J. Curtis, T. J. Kvale, A. Sen, R. M. Schectman, and H. W. Stevens, *Nucl. Instrum. Methods Phys. Res. B* **79**, 746 (1993).
- [45] R. R. Haar and L. J. Curtis, *Nucl. Instrum. Methods Phys. Res. B* **79**, 782 (1993).
- [46] V. S. Nikolaev and I. S. Dimetrev, *Phys. Lett. A* **28**, 277 (1968).
- [47] J. F. Ziegler, J. P. Biersack, and U. Littmark, *The Stopping and Range of Ions in Solids* (Pergamon Press, Oxford, 1985).
- [48] P. Sigmund and K. B. Winterbon, *Nucl. Instrum. Methods Phys. Res.* **119**, 541 (1974).
- [49] L. J. Curtis, H. G. Berry, and J. Bromander, *Phys. Lett.* **34A**, 169 (1971).
- [50] L. J. Curtis, in *Beam Foil Spectroscopy*, edited by S. Bashkin (Springer, Berlin, 1976), pp. 63–109.
- [51] S. W. Provencher, *J. Chem. Phys.* **64**, 2772 (1976).
- [52] L. Engström, *Nucl. Instrum. Methods Phys. Res.* **202**, 369 (1982).